Environmental Science & Technology

pubs.acs.org/est

Article

Molybdenum Bioavailability and Asymbiotic Nitrogen Fixation in Soils are Raised by Iron (Oxyhydr)oxide-Mediated Free Radical Production

Guang-Hui Yu,* Yakov Kuzyakov, Yu Luo, Bernard A. Goodman, Andreas Kappler, Fei-Fei Liu, and Fu-Sheng Sun*

Cite This: *Environ. Sci. Technol.* 2021, 55, 14979−14989

Read Online

ACCESS | Metrics & More | Article Recommendations | Supporting Information

ABSTRACT: Nitrogen (N) fixation in soils is closely linked to microbially mediated molybdenum (Mo) cycling. Therefore, elucidating the mechanisms and factors that affect Mo bioavailability is crucial for understanding N fixation. Here, we demonstrate that long-term (26 years) manure fertilization increased microbial diversity and content of short-range ordered iron (oxyhydr)oxides that raised Mo bioavailability (by 2.8 times) and storage (by ∼30%) and increased the abundance of *nif*H genes (by ∼14%) and nitrogenase activity (by ∼60%). Nanosized iron (oxyhydr)oxides (ferrihydrite, goethite, and hematite nanoparticles) play a dual role in soil Mo cycling: (i) in concert with microorganisms, they raise Mo bioavailability by catalyzing hydroxyl radical ($HO^{\bullet}$) production via the Fenton reactions and (ii) they increase Mo retention by association with the nanosized iron (oxyhydr)oxides. In summary, long-term manure fertilization raised the stock and bioavailability of Mo (and probably also of other micronutrients) by increasing iron (oxyhydr)oxide reactivity and intensified asymbiotic N fixation through an increased abundance of *nif*H genes and nitrogenase activity. This work provides a strategy for increasing biological N fixation in agricultural ecosystems.

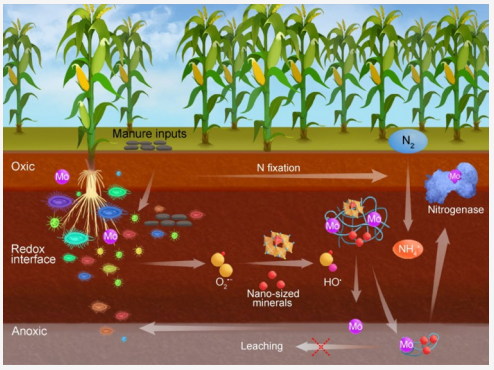

KEYWORDS: *Fenton reaction, hydroxyl radical, iron (oxyhydr)oxide, long-term fertilization, molybdenum bioavailability, nitrogen fixation, reactive oxygen species, stable isotope probing*

INTRODUCTION

Biological nitrogen (N) fixation, which converts dinitrogen (N_2) molecules into bioavailable ammonia (NH_3 or NH_4^+), is the primary biological route for N inputs into Earth's ecosystems.[1−4] Globally, biological N fixation by symbiotic bacteria in higher plants and free-living (asymbiotic) bacteria in soils has been estimated to vary between 44 and 100−300 teragrams (Tg, 1 Tg = 10^{12} g) N yr^{-1}.[1,5−7] Biological N fixation is controlled by the availability of molybdenum (Mo),[1,2,8,9] which is a cofactor of the most common isoform of the N-fixing enzyme nitrogenase (Mo-nitrogenase).[10−12] However, Mo is a limiting nutrient in most terrestrial ecosystems, ranging from tropical and temperate forests to the Arctic.[13−16] In most soils, Mo is rare and susceptible to leaching as soluble Mo(VI) anion molybdate (MoO_4^{2-}) will not be absorbed by negatively charged clay minerals and soil organic matter (SOM).[2] Mo(VI), however, can be abiotically reduced to less soluble Mo(III) by electron transfer from SOM.[17] The formation of strong organic complexes along with adsorption on and coprecipitation with iron (oxyhydr)oxides not only inhibits Mo leaching but also impedes Mo uptake by N-fixing bacteria.[2,15] Therefore, high contents of SOM and highly reactive iron (oxyhydr)oxides (e.g., ferrihydrite [ideal formula $Fe_{10}O_{14}(OH)_2$] with poor crystallinity and large surface area) determine Mo bioavailability.[18]

Analogous to increases in the storage and bioavailability of Mo as a result of leaf litter inputs in forest soils,[2] long-term manure inputs[19,20] may play a critical role in increasing the total content and bioavailability of Mo in agricultural soils. Furthermore, the stimulation of asymbiotic N fixation by manure input can be more important than symbiotic N fixation.[16] Although asymbiotic bacteria have a lower N fixation rate than symbiotic bacteria, the asymbiotic bacteria have a wide distribution globally, are independent on legumes, and fix considerable N amounts in some ecosystems (e.g., deserts and tropical forests).[21] Asymbiotic N fixation is approximately 10−15 kg N ha^{-1} yr^{-1} and accounts for up to

Received: June 28, 2021
Revised: October 7, 2021
Accepted: October 8, 2021
Published: October 22, 2021

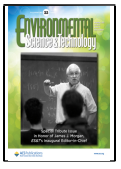

half of all terrestrial N fixation.[7] The N fixation potential is affected by many soil properties, such as Mo bioavailability, SOM content, microbial communities, and so forth. These properties, however, are closely tied to amendments of organic fertilizers, including plant residues and manure. Therefore, understanding of coupling Mo and N cycles is necessary to raise biological N fixation, reduce mineral fertilizer inputs, and stabilize agricultural ecosystems.

We hypothesize that long-term manure input increase Mo stock and bioavailability, and consequently, asymbiotic N fixation in soils. Because taxonomically and ecologically diverse soil microorganisms are an important source of superoxide ($O_2^{\bullet-}$) and hydrogen peroxide (H_2O_2) production under oxic conditions,[22−24] highly reactive iron (oxyhydr)oxides, for example, ferrihydrite, nanosized hematite, and goethite, act as catalysts to decompose H_2O_2 and produce highly oxidative hydroxyl radicals ($HO^{\bullet}$).[25−27] As a nonselective reactive oxygen species (ROS), $HO^{\bullet}$ can oxidize a wide range and variety of organic compounds,[28,29] thus releasing SOM-bound Mo and increasing its bioavailability. To date, the mechanisms controlling the bioavailability of Mo in arable soils and thus biological N fixation remains largely unexplored.

The objectives of this study were (1) to examine whether long-term manure inputs increase the storage and bioavailability of Mo in soil, which further contributes to asymbiotic N fixation; (2) to test whether iron (oxyhydr)oxides in concert with microorganisms increase Mo bioavailability by catalyzing $HO^{\bullet}$ production (Fenton reaction); and (3) to assess the retention of bioavailable Mo by soil constituents, that is, iron (oxyhydr)oxides and SOM. By systematically scrutinizing the effects of long-term (26 years) manure inputs on Mo bioavailability and asymbiotic N fixation in the field and complementary to controlled experiments, our results provide crucial insights into the mechanisms of Mo mobilization in cropland soils to intensify N cycling.

MATERIALS AND METHODS

Study Site and Soil Samples. The well-controlled long-term fertilization experiment was set up in a Ferralic Cambisol in 1990 in Qiyang (26°45′N, 111°52′E), Hunan Province, China. During the period from 1991 to 2016, the mean annual temperature, evaporation, frost-free days, and sunshine hours were 18 °C, 1470 mm, 300 d, and 1610 h, respectively. Prior to the experiment, the field had been under an annual wheat-corn rotation for three years to achieve uniform soil fertility. The mineral fertilizers were urea for nitrogen (N), superphosphate for phosphorus (P), and potassium chloride (KCl) for K. The following fertilization treatments were selected: Control, no fertilization; NPK, mineral N, P, and K fertilization; NPKM, NPK plus pig manure fertilization; M, pig manure alone fertilization. The annual fertilizer amounts applied for the four treatments are provided in Table S1. Lime ($CaCO_3$) was added to the NPK-fertilized fields (so-called NPKCa fertilization) after 2010 to neutralize NPK-induced acidification and to raise the soil pH from ∼4.2 in the NPK-fertilized soil to a pH level similar to the pH in the NPKM soil (∼5.6). The characteristics of pig manure (dry matter) in 2016 were pH 8.5, organic C (364.0 g kg^{-1}), total N (24.0 g kg^{-1}), total Al (9.0 g kg^{-1}), total Fe (5.3 g kg^{-1}), SiO_2 (126 g kg^{-1}), and total Mo (3.5 and 3.4 mg kg^{-1} in the corn and wheat seasons, respectively).

Soils from 0 to 20 cm (Ap horizon) depth were collected in 1990, 1995, 2000, 2005, 2013, and 2016 at the experimental site using a 5 cm diameter auger. Soils at greater depths were also collected at intervals of 20 cm to a maximum depth of 80 cm in 2016. All experimental plots were identically managed with a wheat−corn cropping system.[19] Each plot was 200 m^2 (i.e., 20 m long and 10 m wide), with a 1.0 m deep cement barrier between each plot. Each plot was evenly separated into three regions, and 10 cores were sampled from each region. The collected soils were homogenized by mixing and separated into two parts, one being freeze-dried for DNA extraction and another being air-dried at room temperature, ground, and sieved through a 5-mm sieve for further chemical analyses.

Isotope Tracer Microcosm Experiments. Stable isotope probing (SIP) microcosm experiments were designed: (i) to evaluate the synergistic effects of microbial communities and iron (oxyhydr)oxides on the production of free radicals and (ii) to identify the microbial communities responsible for Fe(III) (oxyhydr)oxide reduction and dissolution as well as $HO^{\bullet}$ formation. Soil slurries from the four fertilization regimes were prepared by mixing the dry soil with distilled water at a ratio of 1:1.[30] To activate the microbes and deplete indigenous electron acceptors such as nitrate, sulfate, and Fe(III) (oxyhydr)oxides, the slurries were further preincubated anaerobically in the dark at 25 °C for 21 d.[30] A PIPES-buffered (10 mM, pH 6.8) artificial ground-water (AGW) medium was used for the soil slurry enrichment culture experiment. The AGW contained 0.11 mM $MgCl_2$, 0.61 mM $CaCl_2$, and 2 mM $NaHCO_3$, 0.5 mM NH_4Cl, 0.05 mM KH_2PO_4, 0.1 × of vitamin and trace element solutions and was supplemented with 11 mM Na-acetate, and 25 mM of hematite. Hematite was synthesized as previously described.[31]

Labeling experiments with the soil slurry enrichment cultures from the four fertilizations (n = 3) were initiated by adding ^{13}C-labeled acetate (99 atom %, Cambridge Isotope Laboratories, MA, USA) as an electron donor, adding hematite as an electron acceptor to each vial at a concentration of 3 mM, and then statically incubating the setups for 8 d at 25 °C. Parallel unlabeled experiments were performed by the same procedure, except that the substrate was unlabeled acetate. Triplicate media in bottles were inoculated with 1% (v/v) soil slurry enrichment cultures as described above. The serum vials were then sealed with butyl rubber septa, flushed with N_2 in the headspaces, and stored in the dark at 25 °C without shaking during incubation periods. Samples of supernatant water and precipitates in triplicate were collected after 8 d incubation from each vial.

Mo Retention Experiments. Mo retention experiments, combined with synchrotron radiation (SR)-based spectroscopic techniques, for example, SR-FTIR and micro-X-ray fluorescence (μ-XRF) spectromicroscopy, were used to examine the components dominating Mo retention in soil. Soil samples from the long-term (26 years) fertilization regimes were mixed with a 100 mg L^{-1} Na_2MoO_4 solution, raised to 100% of water holding capacity, and equilibrated for 24 h at 25 °C.[2] Intact particles were picked using superfine tweezers, frozen at −20 °C, and sectioned without further embedding. A 2 μm thick thin-section was cut on a cryomicrotome (Cyrotome E, Thermo Shandon Limited, UK) and transferred to low-E microscope slides (Kevley Technologies, Ohio, USA). Chemical images of Fe and Mo were collected at beamline 15U1 of the Shanghai Synchrotron Radiation Facility (SSRF) for the same regions of the thin section. Fluorescence maps (μ-XRF) of Mo and Fe were obtained by scanning the samples under a monochromatic

https://doi.org/10.1021/acs.est.1c04240
Environ. Sci. Technol. 2021, 55, 14979−14989

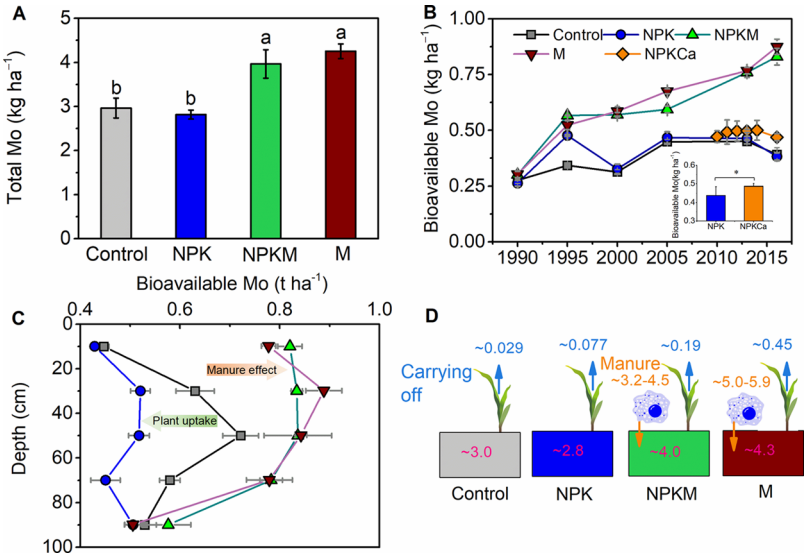

Figure 1. Mo content of soils after long-term (26 years) fertilization. (A) Total Mo in topsoils (0−20 cm) depending on fertilization in 2016. (B) Dynamics of bioavailable Mo during the fertilization period (1990−2016). (C) Changes in bioavailable Mo depending on soil depth (0−100 cm) in 2016. The two arrows show the opposite effects of Mo uptake by plants and Mo addition with manure compared to the unfertilized Control soil. (D) Mo balance depending on fertilization. Blue and orange arrows indicate decreased and increased Mo stocks in soil. Control, no fertilizers; NPK, mineral fertilizers; NPKM, mineral fertilizer plus pig manure; M, pig manure; NPKCa, mineral fertilizer plus lime. Significant differences between fertilization treatments were determined using one-way ANOVA followed by Tukey's HSD post hoc tests at $p < 0.05$, where conditions of normality and homogeneity of variance were met. $n = 3$.

beam at $E = 20$ keV with a step size of 3×3 μm^2 and a dwell time of 5 s.

Acetylene Reduction Activity and *nif*H Genes. Acetylene reduction in samples was measured using the acetylene reduction activity (ARA) method.[10,13] In brief, 100 g of soil (wet mass) was incubated in a jar (1 L) containing 10:1 (v/v) air and acetylene. Gas samples were collected at regular intervals, stored in pre-evacuated serum vials (8 mL), and analyzed by gas chromatography (Shimadzu GC-8A equipped with an FID detector).

Soil DNA was extracted using the PowerMax Soil DNA isolation kit (Mo Bio Laboratories, CA, USA),[32] based on the manufacturer's instructions. The relative abundance of the *nifH* gene was quantified via qPCR. The qPCR assays contained 10 ng of soil DNA, 1.2 μL of each primer (5 pM), 10 μL of 2× SYBR Green iCycler iQ mixture (Bio-Rad), and water for a 20 μL final volume.[33] The assay was carried out on a real-time PCR system (Applied Biosystem 7500) using a program of 95 °C for 10 min, 40 cycles (including 15 s at 95 °C, 20 s at 55 °C, and 20 s at 72 °C). The 16S rRNA gene abundances were applied to normalize values between the samples, and relative quantities were calculated using GENORM software (http://medgen.ugent.be/~jvdesomp/genorm/). The specific primer PolFPolR was used for *nifH*,[33] and all qPCR assays were run in triplicate with soil DNA. To ensure specific assessment of the *nifH* gene, the melting curve in each run was analyzed.

Bacterial Community Analyses. The ^{13}C-labeled DNA was extracted and separated from the natural abundance ^{12}C DNA using density gradient centrifugation and details can be seen in the Supporting Information. To reduce DNA extraction bias, one extract from each of the triplicate bottles in each treatment was performed. In total, three successive DNA extracts from each treatment were pooled. To amplify the V3−V4 region of the 16S rRNA genes, both 338F and 806R primer sets were used as forward primers and reverse primers, respectively.[34] The amplification conditions were as follows: (1) 98 °C for 5 min; (2) 25 cycles of 98 °C for 30 s, 50 °C for 30 s, and 72 °C for 30 s; and (3) a final extension at 72 °C for 5 min. The PCR products were subjected to Illumina MiSeq sequencing after purification by a QIAquick Gel Extraction Kit (Qiagen, CA, USA).[35] In this study, the required sequences were above 150 bp long with a base quality over Q20 and without N bases (fuzzy bases) (Supporting Information). In total, 1,070,823 and 581,032 high-quality sequences were obtained from the 24 isotope tracer incubation samples and 12 field soil samples, respectively. The DNA sequences from all field and incubation samples were deposited in the BIG Data Center, Chinese Academy of Sciences under accession code CRA003592 (https://bigd.big.ac.cn/gsa/browse/CRA003592).

Electron Paramagnetic Resonance and Physico-Chemical Analyses. Analyses of total Mo, bioavailable Mo, H_2O_2, $HO^{\bullet}$, TN, nitrate (NO_3^-), ammonium (NH_4^+), DOC, Fe chemistry, bulk density, and electron paramagnetic resonance (EPR) are provided in the Supporting Information.

Statistical Analysis. One-way analysis of variance (ANOVA) on the soil biogeochemical and taxonomic data was performed using SPSS software (Version 19.0 for Windows). Significances between fertilization treatments were determined using one-way ANOVA and the Tukey's HSD post hoc tests, in which normality and homogeneity of variance were met. The relative percentage of each phylum in the sequencing data was used as their relative abundance. Redundancy analysis (RDA), diversity indices and microbial community richness were determined with the VEGAN package (in R version 3.1.0).

RESULTS

Soil Mo Storage and Bioavailability in Response to Long-Term Fertilization. Long-term manure application (M, NPKM fertilization) increased the total Mo content in the

https://doi.org/10.1021/acs.est.1c04240
Environ. Sci. Technol. 2021, 55, 14979−14989

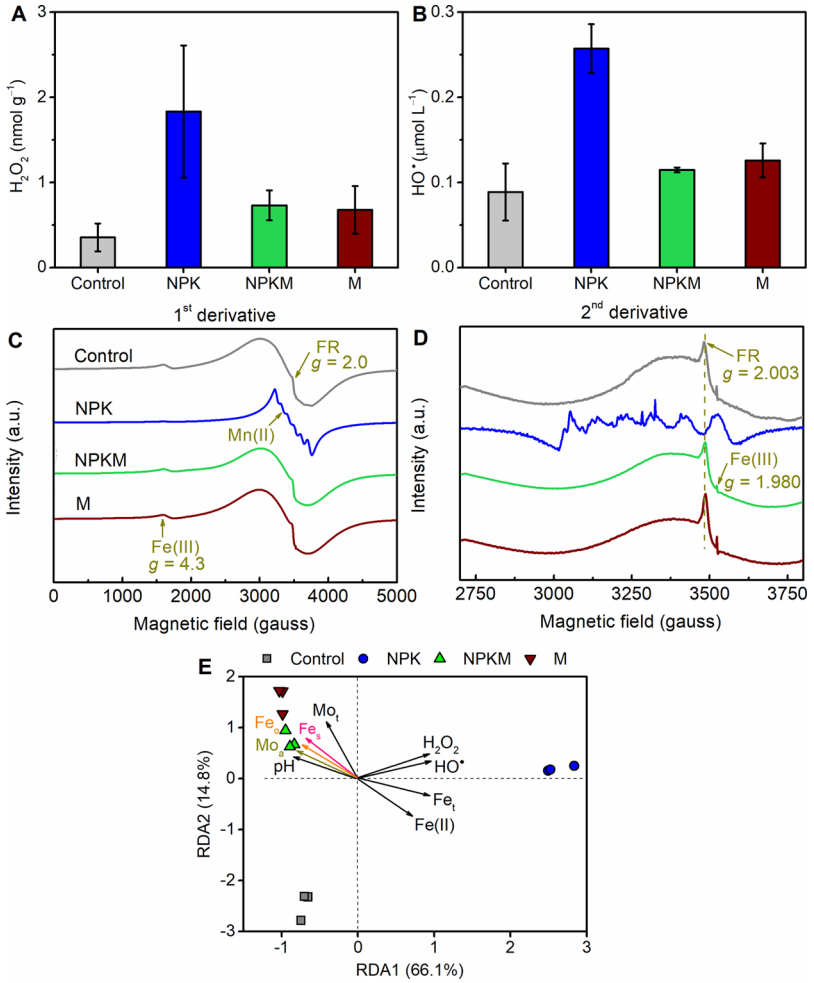

Figure 2. Fenton chemistry and the factors affecting bioavailable Mo in soils after long-term fertilization. (A) H_2O_2 content. (B) HO• generation capacity. (C) 1st derivative and (D) 2nd derivative EPR spectra. (E) RDA of the abundant bacterial phyla and soil properties as well as ROS. Control, no fertilizers; NPK, mineral fertilizers; NPKM, mineral fertilizer plus pig manure; M, pig manure. FR, free radicals. Mo_a, available Mo; Mo_t, total Mo; TN, total nitrogen; Fe_t, total Fe; Fe_s, dissolved Fe; Fe_o, ammonium oxalate extracted Fe. Significant differences between fertilization treatments were determined using one-way ANOVA followed by Tukey's HSD post hoc tests at $p < 0.05$, where conditions of normality and homogeneity of variance were met. $n = 3$.

topsoil (20 cm) by >30%, that is, from ~3 kg ha^{-1} (Control and NPK fertilization) to ~4 kg ha^{-1} (Figure 1A). Remarkably, M and NPKM fertilization increased the bioavailable Mo by >2.8 times in the topsoil, that is, from 0.28 kg ha^{-1} in 1990 to 0.80 kg ha^{-1} in 2016. In contrast, Mo bioavailability in the Control and NPK fertilization regimes increased only slightly (by <0.2 kg ha^{-1}) (Figure 1B). The bioavailable Mo in soils with NPK fertilization increased with lime addition ($p < 0.05$, Figure 1B and Table S2). Except for topsoil, M and NPKM fertilization also increased ($p < 0.05$) the bioavailable Mo up to 60 cm depth when compared to control and NPK fertilization (Figure 1C). Below 80 cm, however, the Mo was independent on fertilization.

During the 26 years of fertilization, Mo was removed from the soil under the control, NPK, NPKM, and M regimes by harvesting grains and straws of approximately 0.029, 0.077, 0.19, and 0.450 kg ha^{-1}, respectively (Figure S1, Table S2, and Supporting Information Results), corresponding to ~1 to 10% of the total Mo content in the soil (top 20 cm). By combining the total Mo remaining in soils (Figure 1A) with the Mo removed by grains and straws (Figure 1D, Table S3, Supplementary Results), our results clearly demonstrate that manure inputs increase the Mo stock in the soil. Compared to nonmanure-fertilized soils, manure-fertilized soils had 37−66 and 54−125% higher contents of oxalate-extractable Fe (i.e., Fe_o) and SOC, respectively (Table S2). Therefore, the increased Mo stock in manure fertilized soils is ascribed to a combination of a direct Mo input from pig manure (see Methods Section, Table S4) and an indirect Mo retention against leaching by increased short-range-ordered (SRO) Fe (oxyhydr)oxide (i.e., Fe_o) and SOC stocks. Notably, a linear positive correlation ($p < 0.05$) between crop yields and bioavailable Mo in the soil (Figure S2, Table S3) suggests that an increase in bioavailable Mo content can contribute to increased crop yields.

Iron (Oxyhydr)oxides Acting as Catalysts to Drive Mo Availability. By producing a strong oxidative HO• radical, the interaction between iron (oxyhydr)oxides and microorganisms via the Fenton oxidation may play an essential role in driving the biogeochemical cycling of Mo. To explore the synergetic mechanisms between Fe (oxyhydr)oxides and microbial communities that affect bioavailable Mo, we first examined H_2O_2, HO•, and Fe chemistry. After 26 years of fertilization, the H_2O_2 and HO• generation capacities were ~2 times higher

https://doi.org/10.1021/acs.est.1c04240
Environ. Sci. Technol. 2021, 55, 14979−14989

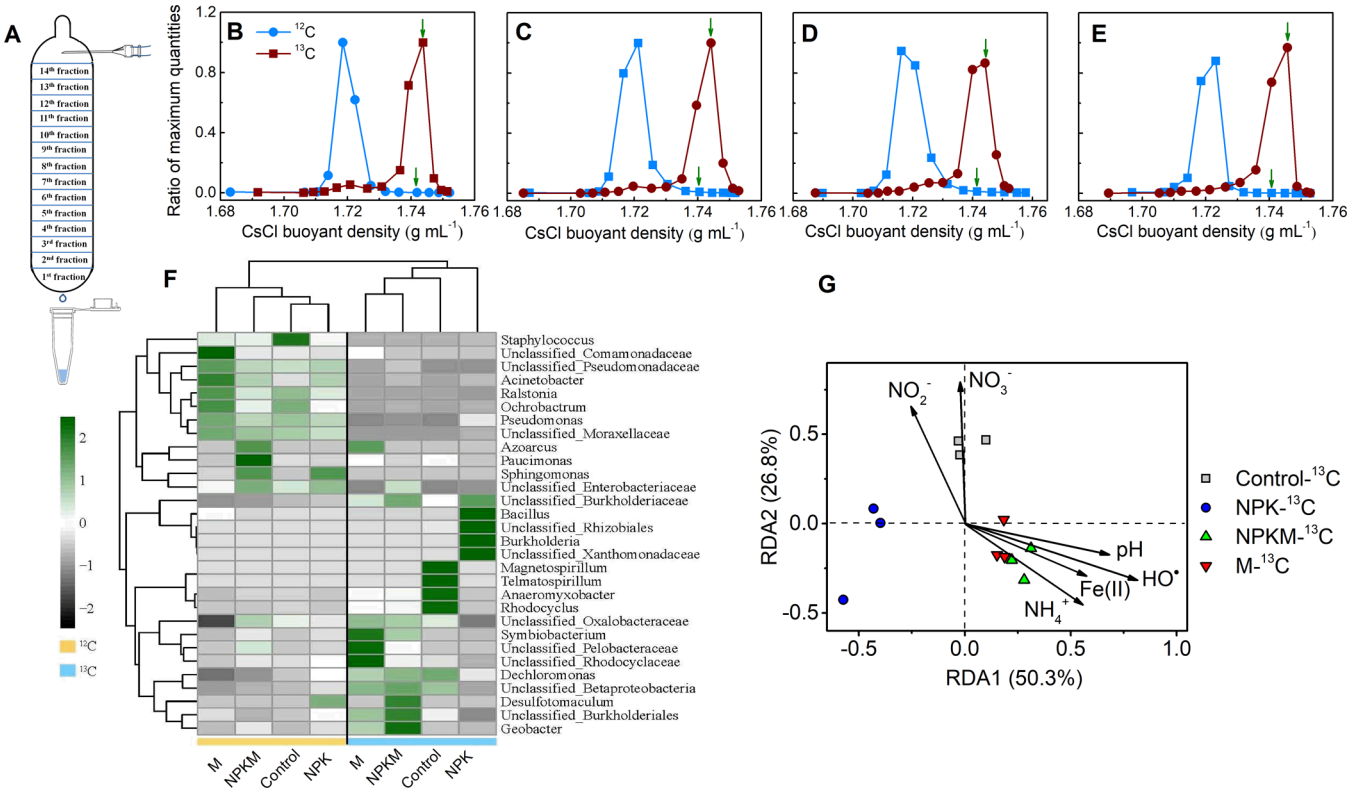

Figure 3. DNA-^{13}C−SIP microcosm experiments illustrating functional microbial communities responsible for Fe(III) (oxyhydr)oxide reduction and dissolution as well as HO• formation. (A) Diagram of SIP. (B−E) Distribution of the relative abundances of functional bacterial genes in the CsCl density gradient for unfertilized (Control), NPK-, NPKM-, and M-fertilized soils after 8 d of incubation. The small green arrows in (B−E) indicate the maximum value for buoyant density. (F) Heat map showing the change in soil bacterial community structure. (G) RDA of the abundant bacterial phyla and environmental variables for individual samples. Control, no fertilizers; NPK, mineral fertilizers; NPKM, mineral fertilizer plus pig manure; M, pig manure. Note the strong difference in microbial groups utilizing ^{12}C and ^{13}C substrates.

in the NPK-fertilized soil than in the control, M and NPKM fertilization treatments (Figure 2A,B). Therefore, free radical reactions, for example, the Fenton or Fenton-like reactions, are stronger in the NPK soil than in the control, M, and NPKM soils. The EPR spectra of the water-dispersible colloidal fractions (presented as 1st and 2nd derivatives, Figure 2C,D) also showed major differences between the paramagnetic components in the NPK soil and those from the other fertilization regimes. Specifically, the control, M and NPKM soils have strong broad signals centered on g = 2.0 from magnetically interacting Fe(III) ions, whereas the spectrum of the NPK soil was dominated by a strong sextet signal from Mn(II). Furthermore, the control, M, and NPKM soils, all showed a free radical signal from environmentally persistent free radicals (EPFRs), with g-factors of ∼2.003, but this signal was much weaker and had a narrower linewidth in the colloidal fraction from the NPK soil. The generation capacity of both H_2O_2 and HO• had a similar trend to total Fe and Fe(II) but was inversely related to dissolved Fe and SRO Fe (oxyhydr)-oxides (Table S2, Figure S3).

High-quality sequencing with RDA was further used to explore relationships between the abundant bacterial phyla and soil properties (Figure 2E). ROS, Fe chemistry, Mo, and pH all significantly (p < 0.01) impacted the bacterial community and explained 80.9% of the variance. The bacterial community compositions in soils with the same fertilization were clustered closely together but clearly bulked by the fertilization regimes. The microbial community structure of both soils with manure was very similar and was affected by the same soil properties, including Mo and Fe contents and pH. Intriguingly, SRO Fe (oxyhydr)oxides (Fe_o) and dissolved Fe were positively correlated with total and bioavailable Mo but negatively correlated with H_2O_2 and HO•; in contrast, total Fe and Fe(II) were positively correlated with H_2O_2 and HO• (Figures 2E and S3). The results from pairwise correlations (Figure S3) suggest that Fe(II) and total Fe are responsible for the occurrence of microbially mediated free radicals, while short-range ordered Fe (oxyhydr)oxides and dissolved Fe contribute to Mo retention.

For further identification of key bacterial communities responsible for Fe(III) reduction and Fe(III) (oxyhydr)oxide dissolution as well as HO• formation, we set up a microcosm study with soil slurry enrichment cultures incubated with ^{13}C-labeled acetate and synthetic hematite. Fe(III) oxide hematite acts as an electron acceptor, whereas acetate and ammonia serve as electron donors. Sequenced 16S ribosomal RNA (rRNA) gene amplicons for genomic DNA were used to identify active bacterial communities (Figure 3). For the unlabeled control soil, the relative abundance of bacterial communities reached the maximum buoyant density of 1.72 g mL^{-1} in the light fractions after 8 days. The relative abundance of bacterial communities in ^{13}C-labeled microcosms, however, peaked in the heavy fractions, that is, with a buoyant density of 1.74 g mL^{-1} (Figure 3B−E). This clear peak shift in the DNA buoyant density indicated that the active bacterial communities assimilated ^{13}C-labeled acetate. The corresponding heat map further displayed the distinct active bacterial groups across all fertilization regimes (Figure 3F): *Azoarcus*, *Pelobacteraceae*,

https://doi.org/10.1021/acs.est.1c04240
Environ. Sci. Technol. 2021, 55, 14979−14989

Burkholderiales (N-fixing), *Geobacter* (dissimilatory iron-reducing), *Symbiobacterium* (symbiotic bacteria), *Rhodocyclaceae* (nitrate-reducing), *Betaproteobacteria* (ammonia-reducing), *Rhodocyclaceae*, and *Oxalobacteraceae* in the manured soil. In the NPKM-fertilized soil, the main active bacterial groups were *Burkholderiales*, *Bulkholderiaceae*, and *Enterobacteriaceae*. In striking contrast, the active bacterial groups were detected as *Anaeromyxobacter* and *Rhodocyclus* in the control soil and *Rhizobiales*, *Bulkholderiaceae* and *Burkholderia* in the NPK soil (Figure 3F). These active bacterial groups in the soil with manure (M and NPKM) drove much more reduction and dissolution of Fe(III) (oxyhydr)oxides as well as formation of $HO^{\bullet}$ than Control and NPK soils (Figure S4). A linear correlation ($R^2 > 0.51$, $p < 0.01$) between $HO^{\bullet}$ and Fe(II) (Figure S5) suggests that Fe(III) reduction contributes to $HO^{\bullet}$ formation, which was related to microbial communities as evidenced by high-quality sequencing with RDA (Figure 3G). Based on the pairwise correlation analysis (Figure S6), the species *Symbiobacterium*, *Geobacter*, *Rhodocyclaceae*, and *Azospirillum*, were closely positively affiliated ($p < 0.01$) with the changes in both $HO^{\bullet}$ and Fe(II). In contrast, the species that were highly negatively affiliated ($p < 0.01$) with both $HO^{\bullet}$ and Fe(II) were *Burkholderia*, *Xanthomonadaceae*, *Rhizobiales*, and *Brevibacillus*. Close spatial colocalization of ^{13}C-labeled carbon ($^{13}C^-$) with iron (oxyhydr)oxides ($^{56}Fe^{16}O^-$ and $^{16}O^-$) (Figure 4) confirms the occurrence of direct microbial mediated electron transport between the donor (i.e., ^{13}C-labeled acetate) and the acceptor (i.e., hematite).

Spectroscopic Insights into Mo Retention by Iron (Oxyhydr)oxides and SOM. Because of the low Mo content in soils, Mo binding sites cannot be observed directly (Figure S7). Thus, the binding of Mo was investigated by mixing the soils with a solution containing 100 mg L^{-1} Na_2MoO_4, followed by equilibration for 24 h at room temperature. Nanoscale secondary ion mass spectrometry (NanoSIMS) images (Figure S8) of the incubated soil water dispersible colloids demonstrated that the iron (oxyhydr)oxides ($^{56}Fe^{16}O^-$) and SOM ($^{12}C^{14}N^-$) in the M soil had a stronger Mo ($^{95}Mo^{16}O^-$) retention capacity than those in other soils. To further visualize the Mo retention by iron (oxyhydr)oxides and SOM, a set of complementary techniques, that is, μ-XRF, SR-FTIR, and electron probe microanalysis (EPMA), was used to map the distribution of Mo, Fe, and organic functional groups in a thin section (~1 μm in thickness) from the manured soil (Figures 5 and S9). Typically, Mo and Fe were heterogeneously distributed in the soil, with several hotspots identified in the brim (Figure 5A,B). There was a strong positive correlation ($R^2 = 0.58$, $p < 0.0001$) between Mo and Fe localization (Figure 5C). This colocalization is supported by high-resolution transmission electron micrograph images and energy dispersive X-ray spectra (Figure S10), which confirm that positive charges of Fe nanoparticles were colocalized with Mo (Figure S10), rather than negative charges of aluminosilicates (Figure S9). Thus, Fe (oxyhydr)oxides play an essential role in Mo retention and prevent its loss via dissolution and leaching.

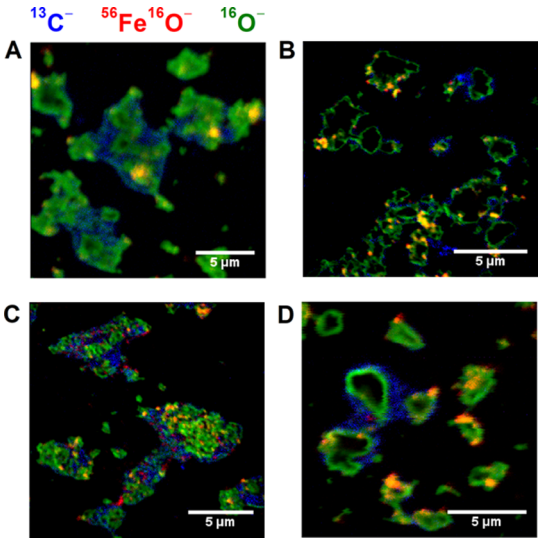

Figure 4. NanoSIMS images showing close spatial colocalization of ^{13}C-labeled carbon ($^{13}C^-$) with iron (oxyhydr)oxides ($^{56}Fe^{16}O^-$ and $^{16}O^-$) confirming the occurrence of direct microbial mediated electron transport between the donor (i.e., ^{13}C-labeled acetate) and the acceptor (i.e., hematite). (A) Control, no fertilizers; (B) NPK, mineral fertilizers; (C) NPKM, mineral fertilizer plus pig manure; (D) M, pig manure. Composite element distribution map of $^{13}C^-$ (blue), $^{56}Fe^{16}O^-$ (red), and $^{16}O^-$ (green) following 8 d incubation in the DNA-SIP microcosm experiments.

In addition to Fe (oxyhydr)oxides, SR-FTIR spectromicroscopy indicates that functional groups from proteins (C═O, 1650 cm^{-1}), lipids (C−H, 2924 cm^{-1}), and polysaccharides (C−OH, 1080 cm^{-1}) may also serve as binding sites for Mo in the soil (Figure S11). To gain further insights into the role of SOM in Mo retention, an exogenic Mo titration experiment was conducted, that is, adding a series of Mo concentrations (i.e., 10−70 ng mL^{-1}) to dissolved organic matter derived from the M and NPK soils and then analyzing their FTIR spectra. The bands of secondary mineral-related peaks (at 1037, 530, 463, and 425 cm^{-1}) in the FTIR spectra of the M soil changed gradually with Mo concentration (Figure 5D), whereas there were only slight changes in the main functional groups from, for example, lipids (2922 cm^{-1}), proteins (1650 and 1550 cm^{-1}), and polysaccharides (1200−1100 cm^{-1}) (Figure S12). In the NPK soil, however, only functional groups (3409 and 1135 cm^{-1}) were markedly changed by the addition of Mo (Figure S12).

To summarize, these spectroscopic observations provide insights into Mo retention in soils depending on fertilization. Iron (oxyhydr)oxides rather than SOM or clay minerals dominated the Mo retention in the M-fertilized soil, whereas Mo was bound solely to SOM in the NPK soil. This difference in Mo retention between the M and NPK fertilization regimes is explained by a higher abundance of SRO Fe (oxyhydr)oxides (i.e., Fe_o) in the manured than in the NPK fertilized soil (Table S2).

Microbial N Fixation in Response to Long-Term Fertilization. In agreement with the increased total and bioavailable Mo stocks in the soils (Figure 6A,B), manure fertilization increased nitrogenase activity by ~60% compared to unfertilized control soil (Figure 6A). As expected, NPK and NPKM fertilization decreased nitrogenase activity by ~70% compared to the control soil. This result highlights that N fixation is suppressed by mineral N inputs. However, nitrogenase activity was ~5 times higher in the M soils than in the NPK and NPKM soils (Figure 6A).

Furthermore, the abundance of *nifH* genes was the highest (~7.3 log copies g^{-1} soil) in the manured soil and the lowest (~6.4 log copies g^{-1} soil) in the NPK soils (Figure 6B), which

https://doi.org/10.1021/acs.est.1c04240
Environ. Sci. Technol. 2021, 55, 14979−14989

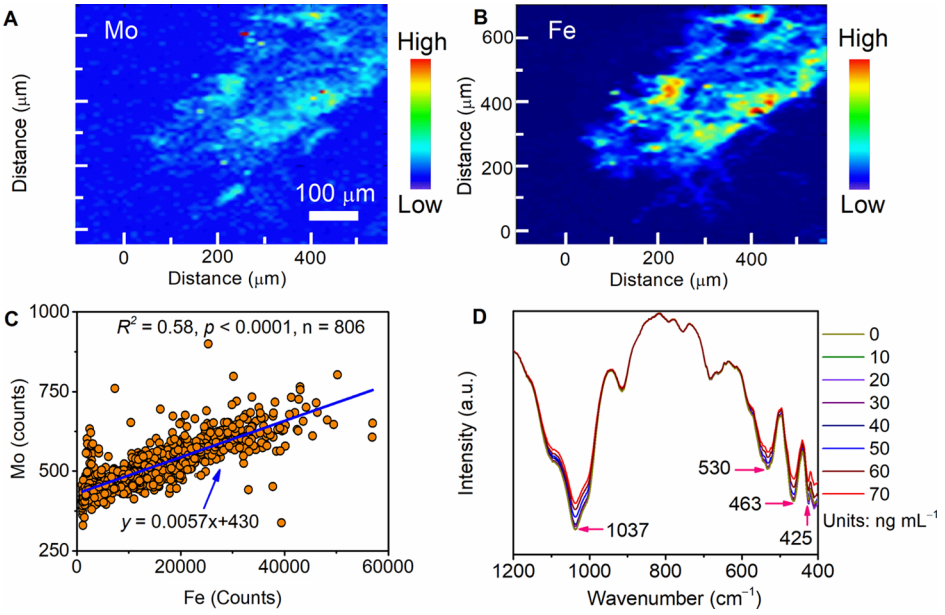

Figure 5. Mo retention by Fe (oxyhydr)oxides in long-term (26 years) pig manure-fertilized soil, M. (A) μ-XRF mapping of Mo. (B) μ-XRF mapping of Fe. (C) Mo vs Fe correlation plot from the (A,B) maps. (D) Response of functional groups in IR spectra to exogenic Mo.

reflects the trends of nitrogenase activity (Figure 6A). Indeed, the abundance of *nifH* genes was similar (~7.0 log copies g^{-1} soil) in soils from both control and NPKM fertilization, indicating that manure inputs can counteract the negative effects of NPK on N-fixing rates. Furthermore, a positive correlation between bioavailable Mo and *nifH* genes but not with ARA (Figure S13) demonstrates that increased Mo availability stimulated N fixation, that is, through the increased N-fixing genes, which could also raise the N-fixing rates (Figure 6C). The independence of ARA from bioavailable Mo (Figure S13) suggests that unlike *nifH* genes, ARA is affected mainly by other soil properties. Together, nitrogenase activity and *nifH* genes abundance analyses provide direct evidence that a long-term manure input (i.e., M fertilization) markedly increases asymbiotic N fixation compared to soils without manure (i.e., control and NPK fertilization).

DISCUSSION

Linking Mo Bioavailability to Microbial N Fixation in Long-Term Fertilized Soils. An increase in Mo storage and bioavailability benefits N fixation by asymbiotic N-fixing bacteria in soils.[13] Manure fertilization markedly increases asymbiotic N fixation in soil (Figure 6) by increasing the stock and bioavailability of Mo (Figure 1) and thus the abundance of *nifH* genes as well as nitrogenase activity (Figures 6A and 5B). This trend is consistent with the previous reports of strong suppression of N fixation by long-term mineral N inputs in tropical forests[13] and agricultural soils.[32] The suppression of N fixation with mineral N inputs may be related to a resulting decrease in the C/N ratio of the soil,[36] increase of mineral N content, functionality losses of keystone and phylogenetically clustered N fixers,[37] and decrease of Mo stock by crop uptake.[11,13,14] Because microorganisms have a relatively stable biomass C/N ratio of 8:1,[38] a stoichiometric theory predicts that a high N content will decrease the transformation rates of immobilized N by microorganisms into microbial biomass N in soils.[36] N fixation was dropped by 50% after 35-years of fertilization, owing to decrease in the abundance of keystone N fixers such as *Geobacter* spp.[37] As a key component of the most common nitrogenase enzyme, Mo bioavailability limits N fixation in tropical forest soils.[11,13]

Factors Determining Mo Bioavailability and Storage in Long-Term Fertilized Soils. The Mo availability strongly decreases with soil acidification.[15] However, Mo bioavailability in the NPKCa soils was only ~57−66% of the Mo bioavailability in the M and NPKM soils (Figure 1B), thus indicating that in addition to soil pH, other factors (e.g., the content of iron (oxyhydr)oxides[39] or SOM[2,15]) may also affect Mo bioavailability. These results were supported by pairwise correlations between soil pH, SRO Fe phases, and dissolved Fe increased (p < 0.05) with bioavailable Mo (Figure S3). Manure input can mobilize iron (oxyhydr)oxides to act as a precursor for nanosized reactive minerals (i.e., ferrihydrite, nanogoethite [α-FeOOH], and hematite [α-Fe_2O_3]) to form SRO phases.[19] Therefore, the SRO Fe phases and dissolved Fe may play an essential role in driving the biogeochemical cycle of Mo (Figures 2 and 3). The bioavailable Mo below 80 cm, however, was independent of fertilization (Figure 1C), which indicates that similar to SOC,[40] the vertical transport of Mo to this depth is of minor importance over 26 years.

Both iron (oxyhydr)oxides and SOM participate in long-term Mo retention and transport from soil.[13,15] Although the Mo(VI) reduction to Mo(III) by SOM represents an important mechanism for its removal from soil solution and uptake by plants and microorganisms,[17] Mo had little affinity to SOM in the long-term fertilized soils (Figures 5 and S12). Our evidence from μ-XRF mapping, FTIR spectra, and TEM images (Figures 5, S10, and S12) strongly demonstrated that mineral surfaces, particularly Fe (oxyhydr)oxides, dominated Mo retention in soils, which is consistent with observation that molybdate (MoO_4^{2-}) is bound mainly to iron (oxyhydr)oxide surfaces.[41] This strong Mo retention capability of nanosized iron (oxyhydr)oxides is explained by their large specific surface area and high proportion of surface atoms (relative to interior atoms).[42]

https://doi.org/10.1021/acs.est.1c04240
Environ. Sci. Technol. 2021, 55, 14979−14989

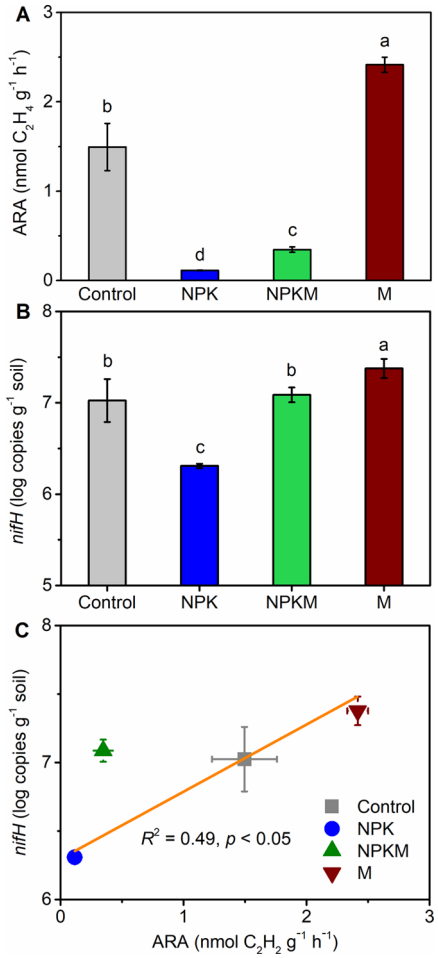

Figure 6. Microbial N fixation in response to long-term fertilization. (A) Nitrogenase ARA. (B) Quantification of *nif*H genes. (C) ARA versus *nif*H genes. Control, no fertilizers; NPK, mineral fertilizers; NPKM, mineral fertilizer plus pig manure; M, pig manure. Significant differences between fertilization treatments were determined using one-way ANOVA followed by Tukey's HSD post hoc tests at $p < 0.05$, where conditions of normality and homogeneity of variance were met. $n = 3$.

Fenton Oxidation and Related Key Microbial Communities. In the long-term fertilized soils, H_2O_2 and HO• increased slightly ($p > 0.05$, except for HO• and total Fe) with total Fe and Fe(II) (Figure S3). The correlation is weak because other soil components (e.g., SOM and minerals) affect the Fenton oxidation.[25,43,44] The SOM and minerals were removed in DNA-SIP microcosm experiments, leading to a very strong positive correlation between HO• and total Fe and Fe(II) (Figure S6). Together, both long-term fertilization and DNA-SIP microcosm experiments indicated that HO• formation is derived from total Fe and Fe(II) oxidation. Furthermore, H_2O_2 and HO• slightly decreased ($p > 0.05$) with increase of dissolved Fe (Fe_s) and SRO Fe (Fe_o) (Figure S3) because they can serve as free radical scavengers. Compared to other soils, a high HO• concentration and thus strong Fenton oxidation in the NPK soil (Figure 2A,B) led to a low Mo stock and bioavailability, owing to its low level of dissolved Fe and SRO Fe. On the one hand, as free radical scavengers, a low content of dissolved Fe and SRO Fe in the NPK soil cannot eliminate HO• (Figure 2B), resulting in much more SOC degradation (Table S2) and then lower binding capacity of total Mo (Figure 1A). On the other hand, as a transient sink of available Mo, a low content of dissolved Fe and SRO Fe cannot retain soluble Mo (Figure S12) and raise Mo bioavailability.

Although the catalytic function of iron oxides in increasing Mo bioavailability has been discovered in the ocean,[22] this discovery has not been extended to soils.[25] The biggest obstacle is the complexity of soil components (including large amounts of free radical scavengers), hindering the direct measurement of hydroxyl radicals in soils.[43] For instance, the reaction rate constants for HO• with DOC, CO_3^{2-}, and Fe^{2+} are ~1.8 to 8.4 × 10^8, 3.7 × 10^8, and 3.5 × 10^8 M^{-1} s^{-1}, respectively.[44] In addition, abundant redox-active minerals in soils can be a sink or a source of HO•, challenging the HO• analyses.[45] In particular, nanosized minerals exhibit unexpected enzyme-like characteristics (named nanozymes), playing key roles in modulating HO• level when interacting with soil microorganisms.[31,45,46] Most recently, the content of hydroxyl radicals in soils was quantified by terephthalic acid (TPA) as a hydroxyl radical trapping agent.[25] However, these common soil components will direct react with HO• and thus enlarge the uncertainty of HO• capture by TPA. To the best of our knowledge, our study provides the first linkage between the Fenton oxidation and Mo bioavailability in soils.

Microbial communities play a central role in the Fenton oxidation in soils by producing superoxide[22−24] and transforming Fe redox cycling.[25,26,31,46] However, the key microbial communities mediating the Fenton oxidation remain unclear. We identified the active bacterial communities (Figure S6), that is, symbiotic *Symbiobacterium*,[47] iron-reducing *Geobacter*,[30] denitrifying bacteria *Rhodocyclaceae*,[48] and N-fixing *Azospirillum*,[49] strongly raising ($p < 0.01$) with HO• and Fe(II) increase. In contrast, N-fixing and iron acquiring *Burkholderia*,[50,51] denitrifier *Xanthomonadaceae*,[52] N-fixing *Rhizobiales*,[1] and *Brevibacillus*[53] strongly decrease ($p < 0.01$) with increasing HO• and Fe(II) concentrations. Although these nitrogen- and iron-cycling species have been extensively reported in soils, we provide the first evidence that the key microbial communities are linked to HO• formation and thus soil Fenton oxidation. Note that these key microbial communities derived from ^{13}C label may be enriched by C transfer from primary to secondary microbial decomposers through cross-feeding.[54] Therefore, the relative contribution of direct feeding from ^{13}C labeled acetate and indirect feeding (cross-feeding) on key microbial communities need to be further investigated by cultivation periods shorter than eight days. Furthermore, these identified key microbial communities related to HO• formation and thus the Fenton oxidation have important implications for ecological and environmental bioremediation of polluted soils (e.g., degrading organic pollutants, mobilizing heavy metals, and oxidation of microplastics[45]).

Environmental Implications. Here, we provide the first field example and detailed mechanisms of the increase in biological N fixation (manifested as ARA and *nif*H genes) due to long-term manure application through increasing Mo stock and bioavailability. This fertilization scheme can be an efficient strategy to increase biological N fixation in agricultural ecosystems. Furthermore, we have revealed a previously unidentified mechanism for increasing Mo bioavailability that is driven by free radical reactions (i.e., Fenton reactions) in soils. These reactions are mediated by the synergy between key microorganisms and Fe (oxyhydr)oxides. Manure inputs can increase short-range-order (SRO) Fe (oxyhydr)oxides by a

https://doi.org/10.1021/acs.est.1c04240
Environ. Sci. Technol. 2021, 55, 14979−14989

"rejuvenation" process in soil.[19,55] Specifically, manure inputs alter Fe-reducing bacterial communities,[20] accelerating Fe cycling in soils, whereas organic acids released from manure or as root exudates transform iron (oxyhydr)oxides from more crystalline to SRO phases.[19] After the formation of SRO (oxyhydr)oxides, these organic acids incorporate into the structure of SRO minerals and prevent their transformation to crystalline forms.[56] Nanosized SRO Fe (oxyhydr)oxides not only serve as catalysts for increasing Mo bioavailability in concert with microorganisms producing increased $HO^{\bullet}$ generation but also play a decisive role for Mo retention. Given naturally occurring iron nanoparticles up to 10^5 Tg in soils[57] and taxonomically and functionally diverse microorganisms being a vast source of superoxide and hydrogen peroxide,[22] we suggest that in addition to strong binding compounds (e.g., siderophores),[58] ROS production may be another widespread microbial strategy to acquire Mo in terrestrial ecosystems.

Based on more than 1 billion large livestock animals in China, producing approximately three billion tons of manure annually,[59] our findings show that manuring should be used to increase biological N fixation in agricultural ecosystems. As a limiting nutrient for N fixation,[11,60] the increased Mo content and bioavailability in soil by manure fertilization is essential for atmospheric N fixation. Our findings have clear implications for organic farming: increased biological N fixation allows for reduction of mineral fertilizers without decreasing crop productivity.[61] Because rock weathering-derived Mo increasingly restricts rates of free-living N fixation,[16,62] our findings suggest that such decoupling of N fixation from net primary productivity by global changes could be partly counteracted by manure fertilization.

■ ASSOCIATED CONTENT

Supporting Information

The Supporting Information is available free of charge at https://pubs.acs.org/doi/10.1021/acs.est.1c04240.

> Mo content in wheat and corn, correlation between bioavailable Mo and crop yields, ppairwise correlations among these physicochemical variables, changes in soil chemical properties during the DNA-SIP microcosm experiment, correlation between $HO^{\bullet}$ generation and total Fe(II), pairwise correlations among the physicochemical variables and functional bacteria, correlative SEM and NanoSIMS images from soils, EPMA, evidence of Mo retention by nanosized Fe (oxyhydr)oxides, synchrotron-based Fourier transform infrared (SR-FTIR) spectromicroscopy, FTIR spectra, ARA and *nifH* genes in soils as a function of bioavailable Mo, fertilizer types and fertilization rates, soil properties, dependence on fertilization regimen of grain and straw yields, and introduced Mo by manure amendments (PDF)

■ AUTHOR INFORMATION

Corresponding Authors

Guang-Hui Yu − *Institute of Surface-Earth System Science, School of Earth System Science, Tianjin Key Laboratory of Earth Critical Zone Science and Sustainable Development in Bohai Rim, Tianjin University, Tianjin 300072, China;* orcid.org/0000-0002-5699-779X; Phone: +86 22 27405053; Email: yuguanghui@tju.edu.cn; Fax: +86-22-27405051

Fu-Sheng Sun − *Institute of Surface-Earth System Science, School of Earth System Science, Tianjin Key Laboratory of Earth Critical Zone Science and Sustainable Development in Bohai Rim, Tianjin University, Tianjin 300072, China;* Email: sunfusheng@tju.edu.cn

Authors

Yakov Kuzyakov − *Department of Soil Science of Temperate Ecosystems, Department of Agricultural Soil Science, University of Göttingen, Göttingen 37073, Germany; Agro-Technological Institute, RUDN University, Moscow 117198, Russia;* orcid.org/0000-0002-9863-8461

Yu Luo − *Institute of Soil and Water Resources and Environmental Science, Zhejiang Provincial Key Laboratory of Agricultural Resources and Environment, Zhejiang University, Hangzhou 310058, China*

Bernard A. Goodman − *College of Physical Science and Technology, Guangxi University, Nanning 530004, China*

Andreas Kappler − *Geomicrobiology, Center for Applied Geosciences, University of Tübingen, Tübingen 72076, Germany; Cluster of Excellence: EXC 2124: Controlling Microbes to Fight Infections, Tübingen 72076, Germany;* orcid.org/0000-0002-3558-9500

Fei-Fei Liu − *College of Resources & Environmental Sciences, Nanjing Agricultural University, Nanjing 210095, China*

Complete contact information is available at: https://pubs.acs.org/10.1021/acs.est.1c04240

Notes

The authors declare no competing financial interest.

■ ACKNOWLEDGMENTS

The authors thank B.R. Wang for his assistance in soil sampling in the Qiyang Long-term Fertilization Station, R.Z. Li, C.C. Huang, Y.Q. Li, and L. Yang for sample analysis, and also the staffs for help and support at beamlines BL15U and BL01B at Shanghai Synchrotron Radiation Facility. This work was supported by the National Natural Science Foundation of China (41977271) and the National Key Research and Development Program of China (2020YFC1806803). Y.K. thanks for the support by the RUDN University Strategic Academic Leadership Program. A.K. acknowledges the infrastructural support by the DFG under Germany's Excellence Strategy, cluster of Excellence EXC2124, project ID 390838134.

■ REFERENCES

(1) Kuypers, M. M. M.; Marchant, H. K.; Kartal, B. The microbial nitrogen-cycling network. *Nat. Rev. Microbiol.* **2018**, *16*, 263−276.

(2) Wichard, T.; Mishra, B.; Myneni, S. C. B.; Bellenger, J.-P.; Kraepiel, A. M. L. Storage and bioavailability of molybdenum in soils increased by organic matter complexation. *Nat. Geosci.* **2009**, *2*, 625−629.

(3) Sun, X.; Kong, T.; Häggblom, M. M.; Kolton, M.; Li, F.; Dong, Y.; Huang, Y.; Li, B.; Sun, W. Chemolithoautotropic diazotrophy dominates the nitrogen fixation process in mine tailings. *Environ. Sci. Technol.* **2020**, *54*, 6082−6093.

(4) Wang, X.; Teng, Y.; Tu, C.; Luo, Y.; Greening, C.; Zhang, N.; Dai, S.; Ren, W.; Zhao, L.; Li, Z. Coupling between nitrogen fixation and tetrachlorobiphenyl dechlorination in a rhizobium-legume symbiosis. *Environ. Sci. Technol.* **2018**, *52*, 2217−2224.

(5) Houlton, B. Z.; Morford, S. L.; Dahlgren, R. A. Convergent evidence for widespread rock nitrogen sources in Earth's surface environment. *Science* **2018**, *360*, 58−62.
(6) Vitousek, P. M.; Menge, D. N. L.; Reed, S. C.; Cleveland, C. C. Biological nitrogen fixation: Rates, patterns and ecological controls in terrestrial ecosystems. *Philos. Trans. R. Soc. Lond. B Biol. Sci.* **2013**, *368*, 20130119.
(7) Sullivan, B. W.; Smith, W. K.; Townsend, A. R.; Nasto, M. K.; Reed, S. C.; Chazdon, R. L.; Cleveland, C. C. Spatially robust estimates of biological nitrogen (N) fixation imply substantial human alteration of the tropical N cycle. *Proc. Natl. Acad. Sci. U.S.A.* **2014**, *111*, 8101−8106.
(8) Bellenger, J.-P.; Wichard, T.; Xu, Y.; Kraepiel, A. M. L. Essential metals for nitrogen fixation in a free-living N_2-fixing bacterium: chelation, homeostasis and high use efficiency. *Environ. Microbiol.* **2011**, *13*, 1395−1411.
(9) Galloway, J. N.; Dentener, F. J.; Capone, D. G.; Boyer, E. W.; Howarth, R. W.; Seitzinger, S. P.; Asner, G. P.; Cleveland, C. C.; Green, P. A.; Holland, E. A.; Karl, D. M.; Michaels, A. F.; Porter, J. H.; Townsend, A. R.; Vöosmarty, C. J. Nitrogen cycles: Past, present, and future. *Biogeochemistry* **2004**, *70*, 153−226.
(10) Bellenger, J. P.; Xu, Y.; Zhang, X.; Morel, F. M. M.; Kraepiel, A. M. L. Possible contribution of alternative nitrogenases to nitrogen fixation by asymbiotic N_2-fixing bacteria in soils. *Soil Biol. Biochem.* **2014**, *69*, 413−420.
(11) Reed, S. C.; Cleveland, C. C.; Townsend, A. R. Relationships among phosphorus, molybdenum and free-living nitrogen fixation in tropical rain forests: Results from observational and experimental analyses. *Biogeochemistry* **2013**, *114*, 135−147.
(12) Darnajoux, R.; Magain, N.; Renaudin, M.; Lutzoni, F.; Bellenger, J.-P.; Zhang, X. Molybdenum threshold for ecosystem scale alternative vanadium nitrogenase activity in boreal forests. *Proc. Natl. Acad. Sci. U.S.A.* **2019**, *116*, 24682−24688.
(13) Barron, A. R.; Wurzburger, N.; Bellenger, J. P.; Wright, S. J.; Kraepiel, A. M. L.; Hedin, L. O. Molybdenum limitation of asymbiotic nitrogen fixation in tropical forest soils. *Nat. Geosci.* **2008**, *2*, 42−45.
(14) Silvester, W. Molybdenum limitation of asymbiotic nitrogen fixation in forests of Pacific Northwest America. *Soil Biol. Biochem.* **1989**, *21*, 283−289.
(15) Marks, J. A.; Perakis, S. S.; King, E. K.; Pett-Ridge, J. Soil organic matter regulates molybdenum storage and mobility in forests. *Biogeochemistry* **2015**, *125*, 167−183.
(16) Dynarski, K. A.; Houlton, B. Z. Nutrient limitation of terrestrial free-living nitrogen fixation. *New Phytol.* **2018**, *217*, 1050−1061.
(17) Goodman, B. A.; Cheshire, M. V. Reduction of molybdate by soil organic matter: EPR evidence for formation of both Mo(V) and Mo(III). *Nature* **1982**, *299*, 618−620.
(18) Guan, X.; Gao, X.; Avellan, A.; Spielman-Sun, E.; Xu, J.; Laughton, S.; Yun, J.; Zhang, Y.; Bland, G. D.; Zhang, Y.; Zhang, R.; Wang, X.; Casman, E. A.; Lowry, G. V. CuO nanoparticles alter the rhizospheric bacterial community and local nitrogen cycling for wheat grown in a Calcareous soil. *Environ. Sci. Technol.* **2020**, *54*, 8699−8709.
(19) Yu, G.; Xiao, J.; Hu, S.; Polizzotto, M. L.; Zhao, F.; McGrath, S. P.; Li, H.; Ran, W.; Shen, Q. Mineral availability as a key regulator of soil carbon storage. *Environ. Sci. Technol.* **2017**, *51*, 4960−4969.
(20) Wen, Y.; Xiao, J.; Liu, F.; Goodman, B. A.; Li, W.; Jia, Z.; Ran, W.; Zhang, R.; Shen, Q.; Yu, G. Contrasting effects of inorganic and organic fertilisation regimes on shifts in Fe redox bacterial communities in red soils. *Soil Biol. Biochem.* **2018**, *117*, 56−67.
(21) Angel, R.; Panhölzl, C.; Gabriel, R.; Herbold, C.; Wanek, W.; Richter, A.; Eichorst, S. A.; Woebken, D. Application of stable-isotope labelling techniques for the detection of active diazotrophs. *Environ. Microbiol.* **2018**, *20*, 44−61.
(22) Diaz, J. M.; Hansel, C. M.; Voelker, B. M.; Mendes, C. M.; Andeer, P. F.; Zhang, T. Widespread production of extracellular superoxide by heterotrophic bacteria. *Science* **2013**, *340*, 1223−1226.
(23) Rineau, F.; Roth, D.; Shah, F.; Smits, M.; Johansson, T.; Canbäck, B.; Olsen, P. B.; Persson, P.; Grell, M. N.; Lindquist, E.; Grigoriev, I. V.; Lange, L.; Tunlid, A. The ectomycorrhizal fungus *Paxillus involutus* converts organic matter in plant litter using a trimmed brown-rot mechanism involving Fenton chemistry. *Environ. Microbiol.* **2012**, *14*, 1477−1487.
(24) Eastwood, D. C.; Floudas, D.; Binder, M.; Majcherczyk, A.; Schneider, P.; Aerts, A.; Asiegbu, F. O.; Baker, S. E.; Barry, K.; Bendiksby, M.; Blumentritt, M.; Coutinho, P. M.; Cullen, D.; de Vries, R. P.; Gathman, A.; Goodell, B.; Henrissat, B.; Ihrmark, K.; Kauserud, H.; Kohler, A.; LaButti, K.; Lapidus, A.; Lavin, J. L.; Lee, Y.-H.; Lindquist, E.; Lilly, W.; Lucas, S.; Morin, E.; Murat, C.; Oguiza, J. A.; Park, J.; Pisabarro, A. G.; Riley, R.; Rosling, A.; Salamov, A.; Schmidt, O.; Schmutz, J.; Skrede, I.; Stenlid, J.; Wiebenga, A.; Xie, X.; Kües, U.; Hibbett, D. S.; Hoffmeister, D.; Högberg, N.; Martin, F.; Grigoriev, I. V.; Watkinson, S. C. The plant cell wall-decomposing machinery underlies the functional diversity of forest fungi. *Science* **2011**, *333*, 762−765.
(25) Du, H.-Y.; Chen, C.-M.; Yu, G.-H.; Polizzotto, M. L.; Sun, F.-S.; Kuzyakov, Y. An iron-dependent burst of hydroxyl radicals stimulates straw decomposition and CO_2 emission from soil hotspots: Consequences of Fenton or Fenton-like reactions. *Geoderma* **2020**, *375*, 114512.
(26) Han, R.; Lv, J.; Huang, Z.; Zhang, S.; Zhang, S. Pathway for the production of hydroxyl radicals during the microbially mediated redox transformation of iron (oxyhydr)oxides. *Environ. Sci. Technol.* **2020**, *54*, 902−910.
(27) Wang, X.; Dong, H.; Zeng, Q.; Xia, Q.; Zhang, L.; Zhou, Z. Reduced iron-containing clay minerals as antibacterial agents. *Environ. Sci. Technol.* **2017**, *51*, 7639−7647.
(28) Wang, B.; Lerdau, M.; He, Y. Widespread production of nonmicrobial greenhouse gases in soils. *Glob. Change Biol.* **2017**, *23*, 4472−4482.
(29) Liao, P.; Li, W.; Jiang, Y.; Wu, J.; Yuan, S.; Fortner, J. D.; Giammar, D. E. Formation, aggregation, and deposition dynamics of NOM-iron colloids at anoxic-oxic interfaces. *Environ. Sci. Technol.* **2017**, *51*, 12235−12245.
(30) Hori, T.; Müller, A.; Igarashi, Y.; Conrad, R.; Friedrich, M. W. Identification of iron-reducing microorganisms in anoxic rice paddy soil by ^{13}C-acetate probing. *ISME J.* **2010**, *4*, 267−278.
(31) Yu, G.-H.; Chi, Z.-L.; Kappler, A.; Sun, F.-S.; Liu, C.-Q.; Teng, H. H.; Gadd, G. M. Fungal nanophase particles catalyze iron transformation for oxidative stress removal and iron acquisition. *Curr. Biol.* **2020**, *30*, 2943−2950.
(32) Feng, J.; Penton, C. R.; He, Z.; Van Nostrand, J. D.; Yuan, M. M.; Wu, L.; Wang, C.; Qin, Y.; Shi, Z. J.; Guo, X.; Schuur, E. A. G.; Luo, Y.; Bracho, R.; Konstantinidis, K. T.; Cole, J. R.; Tiedje, J. M.; Yang, Y.; Zhou, J. Long-term warming in Alaska enlarges the diazotrophic community in deep soils. *mBio* **2019**, *10*, e02521−18.
(33) Collavino, M. M.; Tripp, H. J.; Frank, I. E.; Vidoz, M. L.; Calderoli, P. A.; Donato, M.; Zehr, J. P.; Aguilar, O. M. *nif*H pyrosequencing reveals the potential for location-specific soil chemistry to influence N_2-fixing community dynamics. *Environ. Microbiol.* **2014**, *16*, 3211−3223.
(34) Liu, Y.; Priscu, J. C.; Yao, T.; Vick-Majors, T. J.; Xu, B.; Jiao, N.; Santibáñez, P.; Huang, S.; Wang, N.; Greenwood, M.; Michaud, A. B.; Kang, S.; Wang, J.; Gao, Q.; Yang, Y. Bacterial responses to environmental change on the Tibetan Plateau over the past half century. *Environ. Microbiol.* **2016**, *18*, 1930−1941.
(35) Caporaso, J. G.; Lauber, C. L.; Walters, W. A.; Berg-Lyons, D.; Huntley, J.; Fierer, N.; Owens, S. M.; Betley, J.; Fraser, L.; Bauer, M.; Gormley, N.; Gilbert, J. A.; Smith, G.; Knight, R. Ultra-high-throughput microbial community analysis on the Illumina HiSeq and MiSeq platforms. *ISME J.* **2012**, *6*, 1621−1624.
(36) Li, Z.; Zeng, Z.; Song, Z.; Wang, F.; Tian, D.; Mi, W.; Huang, X.; Wang, J.; Song, L.; Yang, Z.; Wang, J.; Feng, H.; Jiang, L.; Chen, Y.; Luo, Y.; Niu, S. Vital roles of soil microbes in driving terrestrial nitrogen immobilization. *Glob. Change Biol.* **2021**, *27*, 1848−1858.
(37) Fan, K.; Delgado-Baquerizo, M.; Guo, X.; Wang, D.; Wu, Y.; Zhu, M.; Yu, W.; Yao, H.; Zhu, Y.-g.; Chu, H. Suppressed N fixation

https://doi.org/10.1021/acs.est.1c04240
Environ. Sci. Technol. 2021, 55, 14979−14989

and diazotrophs after four decades of fertilization. *Microbiome* **2019**, *7*, 143.
(38) Mooshammer, M.; Wanek, W.; Zechmeister-Boltenstern, S.; Richter, A. Stoichiometric imbalances between terrestrial decomposer communities and their resources: Mechanisms and implications of microbial adaptations to their resources. *Front. Microbiol.* **2014**, *5*, 22.
(39) Goldberg, S.; Forster, H. S.; Godfrey, C. L. Molybdenum adsorption on oxides, clay minerals, and soils. *Soil Sci. Soc. Am. J.* **1996**, *60*, 425−432.
(40) Blanco-Canqui, H.; Hergert, G. W.; Nielsen, R. A. Cattle manure application reduces soil compactibility and increases water retention after 71 years. *Soil Sci. Soc. Am. J.* **2015**, *79*, 212−223.
(41) Lang, F.; Kaupenjohann, M. Immobilisation of molybdate by iron oxides: Effects of organic coatings. *Geoderma* **2003**, *113*, 31−46.
(42) Hochella, M. F.; Mogk, D. W.; Ranville, J.; Allen, I. C.; Luther, G. W.; Marr, L. C.; McGrail, B. P.; Murayama, M.; Qafoku, N. P.; Rosso, K. M.; Sahai, N.; Schroeder, P. A.; Vikesland, P.; Westerhoff, P.; Yang, Y. Natural, incidental, and engineered nanomaterials and their impacts on the Earth system. *Science* **2019**, *363*, No. eaau8299.
(43) Yu, G.-H.; Kuzyakov, Y. Fenton chemistry and reactive oxygen species in soil: Abiotic mechanisms of biotic processes, controls and consequences for carbon and nutrient cycling. *Earth-Sci. Rev.* **2021**, *214*, 103525.
(44) Shaw, T. J.; Luther, G. W., III; Rosas, R.; Oldham, V. E.; Coffey, N. R.; Ferry, J. L.; Dias, D. M. C.; Yücel, M.; de Chanvalon, A. T. Fe-catalyzed sulfide oxidation in hydrothermal plumes is a source of reactive oxygen species to the ocean. *Proc. Natl. Acad. Sci. U.S.A.* **2021**, *118*, No. e2026654118.
(45) Chi, Z.-L.; Yu, G.-H. Nanozyme-mediated elemental biogeochemical cycling and environmental effects. *Sci. China: Earth Sci.* **2021**, *64*, 1015−1025.
(46) Chi, Z. L.; Zhao, X. Y.; Chen, Y. L.; Hao, J. L.; Yu, G. H.; Goodman, B. A.; Gadd, G. M. Intrinsic enzyme-like activity of magnetite particles is enhanced by cultivation with *Trichoderma guizhouense*. *Environ. Microbiol.* **2021**, *23*, 893−907.
(47) Zhang, L.; Jiang, M.; Ding, K.; Zhou, S. Iron oxides affect denitrifying bacterial communities with the *nir*S and *nir*K genes and potential N_2O emission rates from paddy soil. *Eur. J. Soil Biol.* **2019**, *93*, 103093.
(48) Wei, J.-m.; Cui, L.-j.; Li, W.; Ping, Y.-m.; Li, W. Denitrifying bacterial communities in surface-flow constructed wetlands during different seasons: Characteristics and relationships with environment factors. *Sci. Rep.* **2021**, *11*, 4918.
(49) Steenhoudt, O.; Vanderleyden, J. *Azospirillum*, a free-living nitrogen-fixing bacterium closely associated with grasses: Genetic, biochemical and ecological aspects. *FEMS Microbiol. Rev.* **2000**, *24*, 487−506.
(50) Thomas, M. S. Iron acquisition mechanisms of the *Burkholderia cepacia* complex. *BioMetals* **2007**, *20*, 431−452.
(51) Estrada-De Los Santos, P.; Bustillos-Cristales, R.; Caballero-Mellado, J. Burkholderia , a genus rich in plant-associated nitrogen fixers with wide environmental and geographic distribution. *Appl. Environ. Microbiol.* **2001**, *67*, 2790−2798.
(52) Tian, T.; Zhou, K.; Xuan, L.; Zhang, J.-X.; Li, Y.-S.; Liu, D.-F.; Yu, H.-Q. Exclusive microbially driven autotrophic iron-dependent denitrification in a reactor inoculated with activated sludge. *Water Res.* **2020**, *170*, 115300.
(53) Primieri, S.; Dalla Costa, M.; Stroschein, M. R. D.; Stocco, P.; Santos, J. C. P.; Antunes, P. M. Variability in symbiotic effectiveness of N_2 fixing bacteria in Mimosa scabrella. *Appl. Soil Ecol.* **2016**, *102*, 19−25.
(54) Seth, E. C.; Taga, M. E. Nutrient cross-feeding in the microbial world. *Front. Microbiol.* **2014**, *5*, 350.
(55) Raiswell, R. Iron Transport from the Continents to the Open Ocean: The Aging-Rejuvenation Cycle. *Elements* **2011**, *7*, 101−106.
(56) Xu, R. K.; Hu, Y. F.; Dynes, J. J.; Zhao, A. Z.; Blyth, R. I. R.; Kozak, L. M.; Huang, P. M. Coordination nature of aluminum (oxy)hydroxides formed under the influence of low molecular weight organic acids and a soil humic acid studied by X-ray absorption spectroscopy. *Geochim. Cosmochim. Acta* **2010**, *74*, 6422−6435.
(57) Hochell; Michael, F.; Aruguet, D.; Kim, B.; Madden, A. Naturally occurring inorganic nanoparticles: General assessment and a global budget for one of Earth's last unexplored major geochemical components. *Nat. Nanostruct.* **2012**, *1*, 1−42.
(58) Bellenger, J. P.; Wichard, T.; Kustka, A. B.; Kraepiel, A. M. L. Uptake of molybdenum and vanadium by a nitrogen-fixing soil bacterium using siderophores. *Nat. Geosci.* **2008**, *1*, 243−246.
(59) Chadwick, D.; Wei, J.; Yan'an, T.; Guanghui, Y.; Qirong, S.; Qing, C. Improving manure nutrient management towards sustainable agricultural intensification in China. *Agric., Ecosyst. Environ.* **2015**, *209*, 34−46.
(60) Perakis, S. S.; Pett-Ridge, J. C.; Catricala, C. E. Nutrient feedbacks to soil heterotrophic nitrogen fixation in forests. *Biogeochemistry* **2017**, *134*, 41−55.
(61) Bonilla, I.; Bolaños, L. Mineral Nutrition for Legume-Rhizobia Symbiosis: B, Ca, N, P, S, K, Fe, Mo, Co, and Ni: A Review. In *Organic Farming, Pest Control and Remediation of Soil Pollutants: Organic farming, pest control and remediation of soil pollutants*; Lichtfouse, E., Ed.; Springer Netherlands: Dordrecht, 2010; pp 253−274.
(62) Overland, J. E.; Dethloff, K.; Francis, J. A.; Hall, R. J.; Hanna, E.; Kim, S.-J.; Screen, J. A.; Shepherd, T. G.; Vihma, T. Nonlinear response of mid-latitude weather to the changing Arctic. *Nat. Clim. Change* **2016**, *6*, 992−999.

https://doi.org/10.1021/acs.est.1c04240
Environ. Sci. Technol. 2021, 55, 14979−14989